Investigating cryoinjury using simulations and experiments: 1. TF-1 cells during two-step freezing (rapid cooling interrupted with a hold time)

L.U. Ross-Rodriguez[1,2], J.A.W. Elliott[2], L.E. McGann[1†]

[1]Department of Laboratory Medicine and Pathology, University of Alberta, Edmonton, AB, Canada T6G 2R8; [2]Department of Chemical and Materials Engineering, University of Alberta, Edmonton, AB, Canada T6G 2V4

[†]Author to whom correspondence should be addressed. Phone: (780) 431-8764, Fax: (780) 702-2501, Email locksley.mcgann@ualberta.ca.

Keywords

TF-1, computer modeling, simulations, stem cells, cryopreservation, intracellular ice formation

Abstract

There is significant interest in designing a cryopreservation protocol for hematopoietic stem cells (HSC) which does not rely on dimethyl sulfoxide (Me2SO) as a cryoprotectant. Computer simulations that describe cellular osmotic responses during cooling and warming can be used to optimize the viability of cryopreserved HSC; however, a better understanding of cellular osmotic parameters is required for these simulations. As a model for HSC, the erythroleukemic human cell line TF-1 was used in this study. Simulations, based on the osmotic properties of TF-1 cells and on the solution properties of the intra- and extracellular compartments, were used to interpret cryoinjury associated with a two-step cryopreservation protocol. Calculated intracellular supercooling was used as an indicator of cryoinjury related to intracellular ice formation. Simulations were applied to the two-step cooling protocol (rapid cooling interrupted with a hold time) for TF-1 cells in the absence of Me2SO or other cryoprotectants and optimized by minimizing the indicator of cryoinjury. A comparison of simulations and experimental measurements of membrane integrity supports the concept that, for two-step cooling, increasing intracellular supercooling is the primary contributor to potential freezing injury due to the increase in the likelihood of intracellular ice formation. By calculating intracellular supercooling for each step separately and comparing these calculations with cell recovery data, it was demonstrated that it is not optimal simply to limit overall supercooling during two-step freezing procedures. More aptly, appropriate limitations of supercooling differ from the first step to the second step. This study also demonstrates why high cell recovery after cryopreservation could be achieved in the absence of traditional cryoprotectants.

Introduction

Successful transplantation of hematopoietic stem cells (HSC) depends critically on the number of functional cells transplanted. With the range of stem cell applications in transplant medicine recently expanding beyond hematopoietic applications to cardiology [26] and neurology [43], and with the increasing use of umbilical cord blood (CB) as a source for stem cell transplants, the need for adequate quantities of stem cells for various applications has become even more apparent. These applications continue to motivate interest in maximizing recovery of stem cells by more effective means of cryopreservation and storage. Specifically, the use of only clinically-approved reagents while achieving high cell recovery and function requires further investigations.

The current procedures for the cryopreservation of HSC use dimethyl sulfoxide (Me_2SO) to alter the intracellular and extracellular solution properties in order to achieve high recovery after cooling at a constant rate to low temperatures. Even with the widespread use of cryopreserved HSC in autologous transplantation, there is morbidity and mortality associated with the use of Me_2SO [6,11,47,57]. With Me_2SO not being approved for human use in stem cell transplantation, measures have been taken to reduce or eliminate Me_2SO in the cryopreservation process. One approach has been to wash Me_2SO from the product before infusion, resulting in undesirable cell loss [51,56]. While this loss may not be significant for peripheral blood stem cell samples [51] where an excess number of stem cells can be collected from the patient, the number of stem cells is a limiting factor in applications of CB transplants, so additional cell loss due to washing is unacceptable. Other approaches have simply reduced the amount of Me_2SO used in the cryopreservation protocol and there are reports that a minimum of 5 % Me_2SO is necessary for high post-thaw recovery [1,4]. Others have combined a reduced concentration of

Me_2SO with a non-penetrating cryoprotectant such as hydroxyethyl starch (HES) [9,16,20]. In clinical trials, high levels of engraftment were maintained with 3.5 % Me_2SO combined with 5 % HES [16]. While these studies attempted to reduce Me_2SO concentration, the same cooling and warming conditions were used, although it has been demonstrated that the optimal cooling and warming rates depend on the nature and concentration of cryoprotectant [25].

Mazur et al.'s 'two-factor hypothesis' [33] proposed that there are two primary mechanisms of damage during cryopreservation: 1) slow cooling injury related to exposure to high solute concentrations as ice forms and solutes concentrate in the residual liquid, and 2) rapid cooling injury related to the presence of ice inside the cell. The current study uses a two-step cooling procedure as a model for rapid cooling to explore associated cryoinjury. This two-step cooling procedure was described by Farrant et. al. [13,35] as a logical method to investigate the effect of freezing injury on cell recovery. The procedure is based on exposure of cells to a subzero temperature in the presence of extracellular ice for various time intervals before either thawing or rapid cooling to a low storage temperature (-196 °C). This procedure has been used to investigate cryoinjury in several cell types, including hamster lung fibroblasts [14,35], lymphocytes [23], mouse embryos [55], renal cortical slices [5] and islets of Langerhans [3]. Using this procedure [44], we have verified that there is a pattern of cell recovery that is consistent for most cell types. For cells thawed directly from the subzero hold temperature, there is a progressive decline in viability at lower hold temperatures. Furthermore, for cells plunged into liquid nitrogen from the hold temperatures before thawing, cell recovery is low at high subzero hold temperatures, and increases at intermediate hold temperatures. This increase is limited by damage incurred during the first cooling step. It is then possible to differentiate between damage incurred during the first cooling step, including the hold time, and during the

second cooling step. However, our understanding of cryoinjury using empirical studies alone is still limited.

In contrast to purely empirical studies, this study proposes a fundamentally different approach - to reduce or avoid the need for cryoprotectants such as Me_2SO by using solution thermodynamic properties (phase diagrams) and knowledge of osmotic transport to generate temperature profiles that will minimize the major causes of cryoinjury. Computer simulations of cellular responses to low temperatures that are based on mathematical calculations of changes in cell volume have previously been used to further understanding of cellular low temperature responses [10,24,49,50,53]. These models use the osmotic properties of the cell plasma membrane and their temperature dependencies, specific to each cell type, to express theoretical cellular responses to the changes in extracellular osmolality that results from ice formation. The permeability characteristics of the cell membrane regulate water transport and, in turn, intracellular osmolality and intracellular freezing point. Traditionally, cryopreservation protocols have been optimized empirically, but some researchers have explored the use of simulations as a means of predicting low temperature responses of various cell types: bull spermatozoa [53]; bovine erythrocytes [24]; yeast [49]; hamster ova [50]; and corneal epithelial, endothelial and stromal cells [10]. Karlsson et al. developed a theoretical model for predicting intracellular ice formation during cryopreservation by coupling crystal-growth, ice nucleation, and water transport models [19].

In this study, measured osmotic properties of the TF-1 cells were used in simulations of osmotic responses during two-step cooling procedures to minimize supercooling associated with intracellular ice formation. The erythroleukemic human cell line TF-1 is of particular interest as a model for cryopreservation of HSC, since it expresses the $CD34^+$ antigen and is able to

differentiate into the various hematopoietic lineages [21,22,29]. In this study, simulated outcomes were compared to the experimental measurements of TF-1 cell recovery after two-step freezing [44]. In calculating intracellular supercooling, these simulations used non-dilute solution thermodynamic descriptions of the extra- and intracellular solutions to better describe the solution properties at the high concentrations that occur during the two-step freezing procedures. The correlation between freezing experiments and simulations was used to further our understanding of two-step freezing and the cryopreservation of stem cells without Me_2SO.

Simulation specifications

Our simulations of cellular responses at low temperatures used four main elements: 1) the change in the composition of the extracellular solution as ice forms at low temperatures; 2) cellular osmotic responses to changes in composition of the extracellular solution and the resulting change in the composition of the intracellular solution; 3) the temperature dependence of the cellular osmotic permeability parameters; and 4) changes in sample temperature as a function of time.

1) Osmolality of the intracellular and extracellular solutions

Phase diagram information [8,12,54] was used to calculate concentrations in the liquid phase for the extracellular and/or intracellular components (Table 1a). The extracellular components were assumed to be NaCl and KCl, and the intracellular components were assumed to be NaCl, KCl, and protein. Initial concentrations were calculated using the overall concentrations of electrolytes in a mammalian cell [2] and from the isotonic osmolality of the cell (0.3 Osm/kg) and are given in Table 1a. Parameters for the intracellular protein are discussed in the '*Impact of including intracellular protein and nucleation heat'* section, where

simulations with and without intracellular protein are compared. The osmotic virial equation (OVE) [37] was used to describe the osmolality of binary solutions, taking into account the non-ideal behaviour of real solutes:

$$\pi = m + B\,m^2 + C\,m^3 \tag{1}$$

where m is the molality of the solute (moles solute /kg solvent), and B and C are fitting constants for specific solutes in water (Table 1b). For electrolytes, the molality is multiplied by an empirically-determined dissociation constant [39-41]. The constant C in the osmotic virial equation is non-zero only for solutes with highly nonlinear behaviour, such as macromolecules [15,17,42]. The following multisolute OVE, proposed by Elliott et al. [12], was used to calculate osmolality of solutions containing n solutes:

$$\pi = \sum_{i=1}^{n} m_i + \sum_{i=1}^{n}\sum_{j=1}^{n}\left(\frac{B_i + B_j}{2} m_i\, m_j\right) + \sum_{i=1}^{n}\sum_{j=1}^{n}\sum_{k=1}^{n}\left(C_i\, C_j\, C_k\right)^{1/3} m_i\, m_j\, m_k \tag{2}$$

where, in addition to the terms arising from the summation of an Eq. 1 for each solute, Eq. 2 includes terms describing interactions between solutes (i, j and k). The freezing point of the solution is related to the osmolality by:

$$T_{FP} = K_{fp}\,\pi \tag{3}$$

where K_{fp} is the molal freezing point depression constant for water (1.86 °C/(osmole/kg of solvent)).

2) Cellular osmotic responses

The cellular osmotic parameters used in the simulations are the isotonic volume, the hydraulic conductivity, and the osmotically-inactive fraction. Jacobs and Stewart [18] used the following equation to describe the rate of water movement across the plasma membrane :

$$\frac{dV}{dt} = L_p\, A\, R\, T\, (\pi_i - \pi_e)\rho \tag{4}$$

where V is the volume of water in the cell (μm^3), t is the time (min), L_p is the hydraulic conductivity ($\mu m^3/\mu m^2/min/atm$), A is the cell surface area (μm^2), R is the universal gas constant ($\mu m^3 atm/mol/K$), T is the absolute temperature (K), π_e is the extracellular osmolality (osmoles/kg of water), π_i is the intracellular osmolality (osmoles/kg of water), and ρ is the density of water (assumed to be constant at 1.0×10^{-15} kg/μm^3). In these calculations, the cell surface area was calculated from the spherical cell volume, and therefore, assumed to vary with cell volume.

The osmotically-inactive fraction is the fraction of the cell volume not involved in the osmotic activities of the cell. The Boyle van't Hoff relationship [28] was used to express equilibrium cell volume in solutions of impermeant solutes:

$$\frac{V}{V_o} = \frac{\pi^o}{\pi}(1-b) + b \tag{5}$$

where V is the equilibrium cell volume (μm^3) at osmolality π (osmoles/kg water), V_o is the isotonic cell volume (μm^3), π^o is the isotonic osmolality (osmoles/kg water), and b is the osmotically-inactive fraction of the cell volume, a parameter calculated by fitting Eq. 5 to experimental data.

3) Temperature dependence of cellular permeability parameters

Previous studies reported that L_p showed a strong temperature dependence but b did not, so a constant value was assigned for b (Table 1c) [44]. The temperature dependence of L_p is normally described with an Arrhenius relationship [36]:

$$L_p = k\, e^{-\frac{E_a}{RT}} \tag{6}$$

where k is a pre-exponential factor ($\mu m^3/\mu m^2/min/atm$), E_a is the Arrhenius activation energy (kcal/mol), R is the universal gas constant (kcal/mol/K), and T is the absolute temperature (K).

Values for E_a and k [44] are reported in Table 1c. The cellular osmotic parameters for TF-1 cells were previously determined from experimental measurements, varying temperature and osmolality, using an electronic particle counter [44].

4) The temperature profile

The two-step freezing procedure (Figure 1) involves rapidly cooling samples to various subzero hold temperatures, holding at that temperature for a duration ("hold time"), and then either thawing samples directly in a 37 °C water bath (direct thaw) or plunging samples into liquid nitrogen first and then thawing (plunge thaw) [44]. Simulations used the actual measured temperature profiles.

5) Numerical methods

A computer program was developed with the Delphi programming language to perform the calculations in Eqs. 2-6, using Euler's method with sufficiently small discretization to solve the differential equations. Measured temperature profiles in the experimental samples were used in the simulations. Since the cells are initially in osmotic equilibrium with the isotonic extracellular solution, no osmotic changes occur before ice nucleation. The assumptions used in the simulations are a) the simulation begins on ice nucleation at the freezing point of the extracellular solution, b) the extracellular solution remains in equilibrium with extracellular ice. The simulations do not include the formation of intracellular ice; rather, we assume the likelihood of intracellular ice formation increases with supercooling, and therefore use intracellular supercooling as an indicator of the likelihood of intracellular ice formation.

Simulations were performed using measured osmotic parameters of TF-1 cells, i.e. the isotonic cell volume, V_o, the osmotically-inactive fraction, b, the pre-exponential factor, A, and the activation energy, E_a, for L_p, previously described in more detail [44] and listed in Table 1c.

Results of the simulations were compared with previously-reported two-step freezing experimental results for TF-1 cells [44].

Experimental materials and methods

TF-1 cell freezing experiments

Descriptions of the TF-1 cell culture and freezing experiments have been previously reported in detail [44]. Briefly, TF-1 cells (ATCC, Manassas, Virginia) were cultured according to ATCC guidelines. Samples of 0.2 mL TF-1 cell suspension, in serum-free RPMI, in glass tubes (6x50 mm; Fisher, Edmonton, Canada) were transferred into a stirred methanol bath (FTS Systems, Inc., Stone Ridge, New York) preset at -3, -6, -9, -12, -15, -20, or -30 °C and allowed to equilibrate for 2 minutes at that temperature prior to ice nucleation with cold forceps. After nucleation, samples were held at the experimental temperature for 3 minutes before either thawing in a 37 °C water bath or being plunged into liquid nitrogen. Samples were kept in liquid nitrogen for a minimum of 1 hour prior to being thawed in a 37 °C water bath. SYTO®13 (Molecular Probes, Eugene, Oregon) and ethidium bromide (EB) (Sigma, Mississauga, Canada) were used as a cell membrane integrity assay for freeze-thaw injury.

Cooling profiles

Cooling profiles were measured using a Type T thermocouple (Omega, Laval, Canada) in samples paralleling the two-step freezing experiments. Simulations for the two-step freezing technique used measured temperature profiles of the experimental system.

Results and discussion

Two-step cooling simulations

Figure 2 shows the temperature measurements of samples placed in baths at various hold temperatures ranging from -3 °C to -30 °C, nucleated, and then held for 3 minutes prior to rapidly cooling to liquid nitrogen temperature (250 °C/min) (profiles shown to -40 °C). These temperature profiles were used in the simulations, beginning at the freezing point of the solution after ice nucleation, as shown in the inset of Figure 2. The first step and the second (plunge) step of the cooling process, as well as the hold temperatures, are indicated on the figure. Using these temperature profiles and the parameters listed in Table 1, cellular osmotic responses were calculated. Figure 3a shows the calculated cell volumes as a function of time for the corresponding cooling profiles shown in Figure 2. Cell volumes decreased with time during the 3 minute hold, with the degree of shrinkage dependent on the hold temperature. There was a small additional cell shrinkage during the plunge step. Figure 3b shows the calculated cell volumes as a function of temperature, which allows correlation of changes in cell volume with the stage of the cooling protocol. Cell volumes decreased with hold temperature during the hold time, with a small additional decrease during the plunge step.

Figure 4a shows calculated intracellular supercooling as a function of time after nucleation and demonstrates varying degrees of intracellular supercooling during the first cooling step to the hold temperature and during the second step (i.e. supercooling reached in the second step by the time the cells are cooled to -40 °C). For the first step, the lower the hold temperature, the higher the degree of intracellular supercooling. At all hold temperatures there is then a decrease in supercooling during the hold time as water leaves the cell. There is an additional increase in calculated supercooling during the second (plunge) step. Figure 4b shows supercooling as a function of temperature and demonstrates a similar pattern of supercooling for all hold temperatures, with the exception of -3 °C. There is an initial increase in supercooling

during the first step, followed by a decrease to 0 °C supercooling during the hold time, and then followed by another increase in supercooling during the second step. This figure illustrates how the increases in supercooling during each step of the two-step freezing procedure differ for different hold temperatures. This is the direct result of the cell not losing as much water during the previous stages of the cooling profile. Cells are likely to freeze intracellularly at higher degrees of supercooling. The simulations were stopped at -40 °C since it has been suggested previously that when no cryoprotectant is present, injury resulting from exposure to low temperatures occurs at temperatures above -40 °C [14,27], and the accuracy of extrapolating simulations to lower temperatures is questionable.

The maximum supercooling for all the cooling profiles was calculated for each step of the freezing procedure and plotted in Figure 5a (vertical dashed lines indicating three sections are for reference to Figure 5b). There is a progressive increase in the amount of supercooling reached in the first cooling step with decreasing hold temperature, indicating an increased likelihood of intracellular ice formation. There is also a progressive decrease in the amount of supercooling in the second cooling step with decreasing hold temperature, as cells become increasingly dehydrated at the lower hold temperatures before plunging into liquid nitrogen.

Comparison of two-step freezing experiments with simulations

The maximum intracellular supercooling calculated for each step of the cooling profile was used to interpret loss of membrane integrity after two-step cooling experiments. Previously published membrane integrity data as a function of hold temperature for TF-1 cells with a 3 minute hold time [44] are shown in Figure 5b. This figure divides the temperature scale into 3 sections. In section 1, there is minimal loss of membrane integrity for the direct thaw samples; in section 2, there is a decline in membrane integrity for the direct thaw samples with decreasing

hold temperatures; and in section 3, there is no further change in membrane integrity with decreasing hold temperatures. The first section (0 to -9 °C) shows minimal loss of membrane integrity for direct-thaw samples and the corresponding section 1 in Figure 5a shows low maximum supercooling in the first step. TF-1 cells can therefore withstand ~4 °C of supercooling for 3 minutes without loss of membrane integrity. The decrease in membrane integrity at lower subzero temperatures (sections 2 and 3) also corresponds to an increase in supercooling in the first step. The membrane integrity decreases to 20 % at 18 °C of supercooling and there is no further decrease at lower hold temperatures.

The plunge-thaw membrane integrity results could also be interpreted using calculated maximum supercooling in the second step. In section 1 of Figure 5 (0 to -9 °C), high maximum supercooling in the second step corresponded with ~50 % loss of membrane integrity. Section 2 in Figure 5 (-9 to -20 °C) shows an increase in membrane integrity, which is consistent with a decrease in maximum supercooling reached in the second step. However, membrane integrity in this section is limited by damage incurred in the first cooling step, a trend that is continued in section 3 (-20 to -30 °C). Figure 6 shows membrane integrity of plunge-thaw samples as a percentage of the direct-thaw membrane integrity. This analysis demonstrates that, at lower subzero hold temperatures, no additional damage is incurred by the cells during plunge into liquid nitrogen.

An overall comparison between maximum supercooling (Figure 5a) and membrane integrity (Figure 5b) indicates that TF-1 cells can withstand a smaller amount of supercooling in the first step than in the second step. For example, TF-1 cells, with a hold temperature of -20 °C for the first step, and supercooled by a maximum of 18 °C during the first step, have low membrane integrity (~30 %). Conversely, TF-1 cells, with a hold temperature of -15 °C, and

supercooled by a maximum of 21 °C in the second step are less damaged (membrane integrity ~62 %). Based on experimental observations, Mazur and others have proposed that intracellular ice formation occurs when supercooling is between -5 and -15 °C, when extracellular ice is present [31]. In this study, membrane damage associated with intracellular ice formation starts to occur in some cells when intracellular supercooling is greater than ~4 °C supercooling in the first step (at higher temperatures) and ~20 °C in the second step (at lower temperatures). Hence, it is at intermediate hold temperatures (-6 to -15 °C) for a 3 minute hold time that an optimal range of hold temperatures may occur that minimizes the likelihood of intracellular ice formation after both steps of the freezing protocol.

Impact of including intracellular protein and nucleation heat

Solution properties of the cytoplasm are complex and have yet to be elucidated for cells other than red blood cells. We assumed the non-ideality of the solution thermodynamics of the cytoplasm to be attributed to proteins and electrolytes. We also assumed the protein in TF-1 cells to have thermodynamic properties similar to hemoglobin, which are well known. It has been reported that red blood cells contain approximately 7.3 mmol of hemoglobin per kg of intracellular water [8,48,52]. The amount of intracellular protein in nucleated cells has been reported to be more than half the dry weight of the cell [2]. Since the intracellular protein content for TF-1 cells is not known, we used a value of 3.65 mmolal which was 50 % of the molality of hemoglobin in red blood cells. In simulations reported by de Freitas et al. [7], an intracellular protein concentration of 4 mosmol/L was used, which is similar to the concentration used in this study. The inclusion of protein as an intracellular component had a minimal effect on the calculated maximum supercooling in simulations of two-step cooling (Figure 7) [46].

Simulations in this study were based on measured temperature profiles from two-step

freezing experiments that included the effects of nucleation heat. Figure 8a shows an assumed temperature profile (i.e. which does not include the change in temperature associated with the effect of nucleation heat) as a function of time for the various cooling profiles. The effects of the assumed temperature profile and the measured temperature profile on the calculated maximum supercooling are shown in Figure 8b. Using a measured temperature profile, which includes the effects of nucleation heat, changes the calculated maximum supercooling for both steps of the cooling profile only at high subzero hold temperatures [45].

Conclusions

This study uses an approach of calculating supercooling of the cytoplasm in the presence of extracellular ice as an indicator of the likelihood of cryoinjury. A non-dilute solution thermodynamic description [12] of the extra- and intra-cellular solutions was used to calculate intracellular supercooling. Simulations of an empirical approach of two-step freezing were used to examine the role of exposure to subzero hold temperatures and exposure time. A comparison of simulations and experimental measurements of membrane integrity supports the concept that, for two-step cooling, increasing intracellular supercooling is the primary contributor to potential freezing injury due to the increase in the likelihood of intracellular ice formation. These studies also support the upper limit for tolerable intracellular supercooling previously reported by others during the first step of cooling [30,32,38]. However, a comparison of experimental data with simulations showed that TF-1 cells were able to withstand considerably higher degrees of supercooling in the second step than during the first step.

Supercooling appears to play a determining role in cell recovery in two-step cryopreservation protocols, particularly for cells plunged from high subzero hold temperatures.

By calculating intracellular supercooling for each step separately and comparing these calculations with cell recovery data, it was demonstrated that it is not optimal simply to limit overall supercooling during two-step freezing procedures. More aptly, appropriate limitations of supercooling differ from the first step to the second step. Since water movement across the cell membrane is temperature-dependent, cells need to be exposed to conditions (i.e. subzero hold temperatures) that allow sufficient osmotic water efflux from the cell before cooling to lower subzero temperatures, to prevent high supercooling and the likelihood of intracellular ice formation. During the hold step at high subzero hold temperatures, the incidence of intracellular ice formation is low because supercooling is low. However, during the subsequently plunge step, the amount of supercooling is high because of limited water loss prior to the plunge step. At intermediate subzero hold temperatures, more extracellular ice forms so there is greater water loss. However, due to the lower temperature, supercooling increases. During the plunge step, the additional supercooling before cells reach -40 °C is low thus decreasing the chance of intracellular ice formation. Therefore, in order to ensure that cells are sufficiently dehydrated before the plunge step, cells must be exposed to higher amounts of supercooling at higher subzero hold temperatures. The trend for the intermediate subzero hold temperatures continues for the lower subzero hold temperature range. The proposed target hold temperature determined from experimental results was suggested to be between -6 °C and -15 °C [44], corresponding to a maximum supercooling of less than 10 °C in the first step. In this study using TF-1 cells, calculated supercooling greater than ~4 °C in the first step and ~20 °C in the second step resulted in membrane damage.

Based on the sensitivity analysis, the inclusion of protein, as an intracellular component, minimally affected maximum supercooling. This is not surprising as supercooling depends on

the osmolality of the cytoplasm and not the concentration of the individual components (i.e. protein concentration) that contribute to that osmolality. Also, using an assumed temperature profile, instead of a measured temperature profile (i.e. including the effects of nucleation heat) in this experimental set-up, changes the calculated maximum supercooling for both steps of the cooling profile at high subzero hold temperatures. This change was minimal, so it would be acceptable to neglect the effects of nucleation heat for two-step simulations without cryoprotectant for small volume systems (such as the 0.2 mL volumes used in this study). However for larger systems, with significantly higher latent heat of fusion, the measured temperature profile should be used.

This study demonstrates the usefulness of simulations, combined with two-step freezing experiments, in attempting to provide understanding into the complexities of establishing cryopreservation protocols for a particular cell type. Specifically, two-step freezing provides useful insight into the mechanisms of damage inflicted by cooling over a range of subzero temperatures [34], allowing manipulation of different variables of the cryopreservation protocol for any cell type for which the osmotic parameters are known. The implications for this work extend beyond TF-1 and stem cells, to any cell type with known osmotic parameters. This study also demonstrates the value of a combination of theoretical and empirical work for interpretation of cryopreservation protocols. Based on the results presented in this work, the use of rapid non-linear cooling profiles were integral to understanding the successful results for the cryopreservation of TF-1 cells without Me_2SO.

Acknowledgements

This research was funded by the Canadian Institutes for Health Research (CIHR; MOP

85068, 86492 and CPG 75237) and the Natural Sciences and Engineering Research Council (NSERC) of Canada. J. A. W. Elliott holds a Canada Research Chair in Interfacial Thermodynamics.

References

[1] J.F. Abrahamsen, A.M. Bakken, and O. Bruserud, Cryopreserving human peripheral blood progenitor cells with 5-percent rather than 10-percent DMSO results in less apoptosis and necrosis in CD34+cells. Transfusion 42 (2002) 1573-1580.

[2] B. Alberts, D. Bray, J. Lewis, M. Raff, K. Roberts, and J.D. Watson, Molecular biology of the cell, Garland Publishing, Inc, New York & London, 1994.

[3] H.L. Bank, and L. Reichard, Cryogenic preservation of isolated islets of Langerhans: two-step cooling. Cryobiology 18 (1981) 489-96.

[4] F. Beaujean, J.H. Bourhis, C. Bayle, H. Jouault, M. Divine, C. Rieux, M. Janvier, C. Le Forestier, and J.L. Pico, Successful cryopreservation of purified autologous CD34(+) cells: influence of freezing parameters on cell recovery and engraftment. Bone Marrow Transplant. 22 (1998) 1091-1096.

[5] P. Clark, H.E. Hawkins, and A.M. Karow, The Influence of Temperature on the Function of Renal Cortical Slices Frozen in Various Cryoprotectants. Cryobiology 22 (1985) 156-160.

[6] J.M. Davis, S.D. Rowley, H.G. Braine, S. Piantadosi, and G.W. Santos, Clinical toxicity of cryopreserved bone-marrow graft infusion. Blood 75 (1990) 781-786.

[7] R.C. de Freitas, K.R. Diller, J.R. Lakey, and R.V. Rajotte, Osmotic behavior and transport properties of human islets in a dimethyl sulfoxide solution. Cryobiology 35 (1997) 230-239.

[8] D.A.T. Dick, and L.M. Lowenstein, Osmotic equilibria in human erythrocytes studied by immersion refractometry. Proceedings of the Royal Society of London Series B-Biological Sciences 148 (1958) 241-256.

[9] C. Donaldson, W.J. Armitage, P.A. DenningKendall, A.J. Nicol, B.A. Bradley, and J.M. Hows, Optimal cryopreservation of human umbilical cord blood. Bone Marrow Transplant.

18 (1996) 725-731.

[10] S.L. Ebertz, and L.E. McGann, Osmotic parameters of cells from a bioengineered human corneal equivalent and consequences for cryopreservation. Cryobiology 45 (2002) 109-117.

[11] M.J. Egorin, D.M. Rosen, R. Sridhara, L. Sensenbrenner, and M. Cottler-Fox, Plasma concentrations and pharmacokinetics of dimethylsulfoxide and its metabolites in patients undergoing peripheral-blood stem-cell transplants. Journal of Clinical Oncology 16 (1998) 610-615.

[12] J.A.W. Elliott, R.C. Prickett, H.Y. Elmoazzen, K.R. Porter, and L.E. McGann, A multi-solute osmotic virial equation for solutions of interest in biology. Journal of Physical Chemistry B 111 (2007) 1775-1785.

[13] J. Farrant, S.C. Knight, L.E. McGann, and J. O'Brien, Optimal recovery of lymphocytes and tissue culture cells following rapid cooling. Nature 249 (1974) 452-3.

[14] J. Farrant, C.A. Walter, H. Lee, and L.E. McGann, Use of two-step cooling procedures to examine factors influencing cell survival following freezing and thawing. Cryobiology 14 (1977) 273-286.

[15] J. Gaube, A. Pfennig, and M. Stumpf, Vapor-liquid equilibrium in binary and ternary aqueous solutions of poly(ethylene glycol) and dextran. J. Chem. Eng. Data 38 (1993) 163-166.

[16] P. Halle, O. Tournilhac, W. Knopinska-Posluszny, J. Kanold, P. Gembara, N. Boiret, C. Rapatel, M. Berger, P. Travade, S. Angielski, J. Bonhomme, and F. Demeocq, Uncontrolled-rate freezing and storage at-80 degrees C, with only 3.5-percent DMSO in cryoprotective solution for 109 autologous peripheral blood progenitor cell transplantations. Transfusion 41 (2001) 667-673.

[17] C.A. Haynes, R.A. Beynon, R.S. King, H.W. Blanch, and J.M. Prausnitz, Thermodynamic properties of aqueous polymer solutions: poly(ethylene glycol)/Dextran. J. Phys. Chem. 93 (1989) 5612-5617.

[18] M.H. Jacobs, and D.R. Stewart, A simple method for the quantitative measurement of cell permeability. J. Cell. Comp. Physiol. 1 (1932) 71-82.

[19] J.O.M. Karlsson, E.G. Cravalho, and M. Toner, A model of diffusion-limited ice growth inside biological cells during freezing. Journal of Applied Physics 75 (1994) 4442-4445.

[20] Y. Katayama, T. Yano, A. Bessho, S. Deguchi, K. Sunami, N. Mahmut, K. Shinagawa, E. Omoto, S. Makino, T. Miyamoto, S. Mizuno, T. Fukuda, T. Eto, T. Fujisaki, Y. Ohno, S. Inaba, Y. Niho, and M. Harada, The effects of a simplified method for cryopreservation and thawing procedures on peripheral blood stem cells. Bone Marrow Transplant. 19 (1997) 283-287.

[21] T. Kitamura, T. Tange, T. Terasawa, S. Chiba, T. Kuwaki, K. Miyagawa, Y.F. Piao, K. Miyazono, A. Urabe, and F. Takaku, Establishment and characterization of a unique human cell line that proliferates dependently on GM-CSF, IL-3, or erythropoietin. J. Cell. Physiol. 140 (1989) 323-34.

[22] T. Kitamura, A. Tojo, T. Kuwaki, S. Chiba, K. Miyazono, A. Urabe, and F. Takaku, Identification and analysis of human erythropoietin receptors on a factor-dependent cell-line, TF-1. Blood 73 (1989) 375-380.

[23] S.C. Knight, J. Farrant, and L.E. McGann, Storage of human lymphocytes by freezing in serum alone. Cryobiology 14 (1977) 112-5.

[24] S.P. Leibo, Freezing damage of bovine erythrocytes - simulation using glycerol concentration changes at subzero temperatures. Cryobiology 13 (1976) 587-598.

[25] S.P. Leibo, J. Farrant, P. Mazur, M.G. Hanna, Jr., and L.H. Smith, Effects of freezing on marrow stem cell suspensions: interactions of cooling and warming rates in the presence of PVP, sucrose, or glycerol. Cryobiology 6 (1970) 315-32.

[26] A.C. Lindsay, and J.P. Halcox, Stem cells as future therapy in cardiology. Hosp. Med. 66 (2005) 215-20.

[27] J.E. Lovelock, The mechanism of the protective action of glycerol against haemolysis by freezing and thawing. Biochim Biophys Acta 11 (1953) 28-36.

[28] B. Lucke, and M. McCutcheon, The living cell as an osmotic system and its permeability to water. Physiol. Rev. 12 (1932) 68-139.

[29] M. Marone, G. Scambia, G. Bonanno, S. Rutella, D. de Ritis, F. Guidi, G. Leone, and L. Pierelli, Transforming growth factor-beta 1 transcriptionally activates CD34 and prevents induced differentiation of TF-1 cells in the absence of any cell-cycle effects. Leukemia 16 (2002) 94-105.

[30] P. Mazur, Kinetics of water loss from cells at subzero temperatures and the likelihood of intracellular freezing. J. Gen. Physiol. 47 (1963) 347-69.

[31] P. Mazur, The role of cell membranes in the freezing of yeast and other cells. Annals of the New York Academy of Sciences 125 (1965) 658-676.

[32] P. Mazur, Role of intracellular freezing in death of cells cooled at supraoptimal rates. Cryobiology 14 (1977) 251-272.

[33] P. Mazur, S.P. Leibo, and E.H. Chu, A two-factor hypothesis of freezing injury. Evidence from Chinese hamster tissue-culture cells. Exp. Cell Res. 71 (1972) 345-55.

[34] L.E. McGann, Optimal temperature ranges for control of cooling rate. Cryobiology 16 (1979) 211-6.

[35] L.E. McGann, and J. Farrant, Survival of tissue culture cells frozen by a two-step procedure to -196 degrees C. I. Holding temperature and time. Cryobiology 13 (1976) 261-268.

[36] J.J. Mcgrath, Membrane transport proteins. in: J.J. Mcgrath, and K.R. Diller, (Eds.), Low temperature biotechnology emerging applications and engineering contributions, The American Society of Mechanical Engineers, New York, 1988, pp. 273-330.

[37] W.G. McMillan, and J.E. Mayer, The Statistical Thermodynamics of Multicomponent Systems. J. Chem. Phys. 13 (1945) 276-305.

[38] K. Muldrew, and L.E. McGann, Mechanisms of intracellular ice formation. Biophysical Journal 57 (1990) 525-532.

[39] R.H. Petrucci, and W.S. Harwood, General Chemistry: principles and modern applications, Prentice-Hall, Upper Saddle River, New Jersey, USA, 2007.

[40] R.C. Prickett, J.A.W. Elliott, and L.E. McGann, Application of multisolute osmotic virial equation to solutions containing electrolytes. Cryobiology (submitted) (2010).

[41] R.C. Prickett, J.A.W. Elliott, and L.E. McGann, Application of the osmotic virial equation in cryobiology. Cryobiology 60 (2010) 30-42.

[42] S.J. Rathbone, C.A. Haynes, H.W. Blanch, and J.M. Prausnitz, Thermodynamic properties of dilute aqueous polymer solutions from low-angle laser-light-scattering measurements. Macromolecules 23 (1990) 3944-3947.

[43] C.M. Rice, C.A. Halfpenny, and N.J. Scolding, Stem cells for the treatment of neurological disease. Transfus. Med. 13 (2003) 351-61.

[44] L.U. Ross-Rodriguez, J.A.W. Elliott, and L.E. McGann, Characterization of cryobiological responses in TF-1 cells using interrupted freezing procedures. Cryobiology 60 (2010) 106-116.

[45] L.U. Ross-Rodriguez, J.A.W. Elliott, and L.E. McGann, Investigating cryoinjury using simulations and experiments: 2. TF-1 cells graded freezing (interrupted slow cooling without hold time). Cryobiology (accepted) (2010).

[46] L.U. Ross-Rodriguez, H. Yang, J.A.W. Elliott, and L.E. McGann, Solution properties of the cytoplasm in simulations of cryopreservation protocols. Cell Preservation Technology 2 (2004) 242.

[47] N.C. Santos, J. Figueira-Coelho, J. Martins-Silva, and C. Saldanha, Multidisciplinary utilization of dimethyl sulfoxide: pharmacological, cellular, and molecular aspects. Biochem. Pharmacol. 65 (2003) 1035-1041.

[48] D. Savitz, V.W. Sidel, and A.K. Solomon, Osmotic Properties of Human Red Cells. Journal of General Physiology 48 (1964) 79-94.

[49] G.J. Schwartz, and K.R. Diller, Osmotic response of individual cells during freezing .1. Experimental volume measurements. Cryobiology 20 (1983) 61-77.

[50] M. Shabana, and J.J. Mcgrath, Cryomicroscope investigation and thermodynamic modeling of the freezing of unfertilized hamster ova. Cryobiology 25 (1988) 338-354.

[51] R. Syme, M. Bewick, D. Stewart, K. Porter, T. Chadderton, and S. Gluck, The role of depletion of dimethyl sulfoxide before autografting: on hematologic recovery, side effects, and toxicity. Biol. Blood Marrow Transplant. 10 (2004) 135-41.

[52] F.T. Williams, C.C. Fordham, III, W. Hollander, Jr., and L.G. Welt, A Study of the Osmotic Behaviour of the Human Erythrocyte. Journal of Clinical Investigation 38 (1959) 1587-98.

[53] H. Woelders, and A. Chaveiro, Theoretical prediction of 'optimal' freezing programmes. Cryobiology 49 (2004) 258-271.

[54] J. Wolfe, and G. Bryant, Freezing, drying, and/or vitrification of membrane- solute-water

systems. Cryobiology 39 (1999) 103-129.

[55] M.J. Wood, and J. Farrant, Preservation of mouse embryos by two-step freezing. Cryobiology 17 (1980) 178-80.

[56] H. Yang, Effects of incubation temperature and time after thawing on viability assessment of peripheral hematopoietic progenitor cells cryopreserved for transplantation. Bone Marrow Transplant. 32 (2003) 1021-1026.

[57] A. Zambelli, G. Poggi, G. Da Prada, P. Pedrazzoli, A. Cuomo, D. Miotti, C. Perotti, P. Preti, and G.R. Della Cuna, Clinical toxicity of cryopreserved circulating progenitor cells infusion. Anticancer Res. 18 (1998) 4705-4708.

Figure captions

Figure 1. A schematic of two-step freezing, including initial rapid non-linear cooling to hold temperature, hold time, and either directly thawing (1st step), or plunging, and then thawing (2nd step), following storage time [44].

Figure 2. Simulation input temperature as a function of time, measured post-nucleation during equilibration at various subzero hold temperatures (-3°C to -30°C) for 3 minutes, prior to rapid cooling (250°C/min). The nucleation and hold step (1st step), and the plunge step (2nd step) are indicated on the graph. The figure insert shows the entire measured temperature profile including prior to the nucleation step for one set of experimental conditions.

Figure 3. Calculated relative cell volume as a function of (a) time after nucleation and (b) temperature for TF-1 cells cooled according to the temperature profiles in Figure 2.

Figure 4. Calculated intracellular supercooling as a function of (a) time after nucleation and (b) temperature for TF-1 cells cooled according to the temperature profiles in Figure 2. "Max" indicates where the maximum supercooling occurs during the 1st and 2nd steps (for simulations down to -40 °C, where simulations were stopped) for a particular hold temperature.

Figure 5. (a) Maximum intracellular supercooling during the 1st step (solid line) and the 2nd step (dotted line) as a function of hold temperature for TF-1 cells (for simulations down to -40 °C). Vertical dashed lines indicating three sections for comparison with Figure 5b. (b) Membrane integrity for TF-1 cells (±SEM; normalized to controls) in serum-free RPMI following two-step freezing with a 3 minute hold time and includes sections on the figure where loss of membrane integrity is a result of either supercooling in the 1st or 2nd step, or both, of the two-step freezing procedure [44].

Figure 6. Membrane integrity for TF-1 cells (±SEM; normalized to controls) in serum-free

RPMI following two-step freezing with a 3 minute hold time and includes a plunge-thaw curve normalized with (i.e. as a percentage of) the direct-thaw data (long dashes).

Figure 7. Cell model with and without intracellular protein. Maximum intracellular supercooling during the 1st step (solid line) and the 2nd step (dotted line) as a function of hold temperature for TF-1 cells.

Figure 8. Effect of using an assumed temperature profile rather than a measured temperature profile which includes nucleation heat. (a) Simulation input temperature as a function of time and (b) the corresponding calculated maximum supercooling during the 1st step (solid line) and the 2nd step (dotted line) as a function of hold temperature for TF-1 cells.

Table 1. Parameters used in simulations: (a) isotonic solution composition, (b) solution parameters, and (c) osmotic parameters for TF-1 cells

a) Isotonic solution composition

	Extracellular	Intracellular
NaCl	0.170 molal	0.010 molal
KCl	0.005 molal	0.133 molal
Protein	0	0.004 molal
Total Osmolality	0.300 Osm/kg	0.300 Osm/kg

b) Solution parameters [12]

	B (mol/kg solvent)$^{-1}$	C (mol/kg solvent)$^{-2}$	K
NaCl	0.02986	0	1.702
KCl	0	0	1.742
Protein†	49.3	3.07×10^4	1

c) Osmotic parameters [45]

Isotonic volume, V_o	916 μm^3
Inactive fraction, b	0.361
E_a (Activation Energy for L_p)	14.2 kcal/mol
k (Pre-exponential factor for L_p)	1.33×10^{10} $\mu m^3/\mu m^2$/min/atm

†based on values reported for hemoglobin
L_p is the hydraulic conductivity
B is the second osmotic virial coefficient
C is the third osmotic virial coefficient
K is the dissociation constant for electrolytes

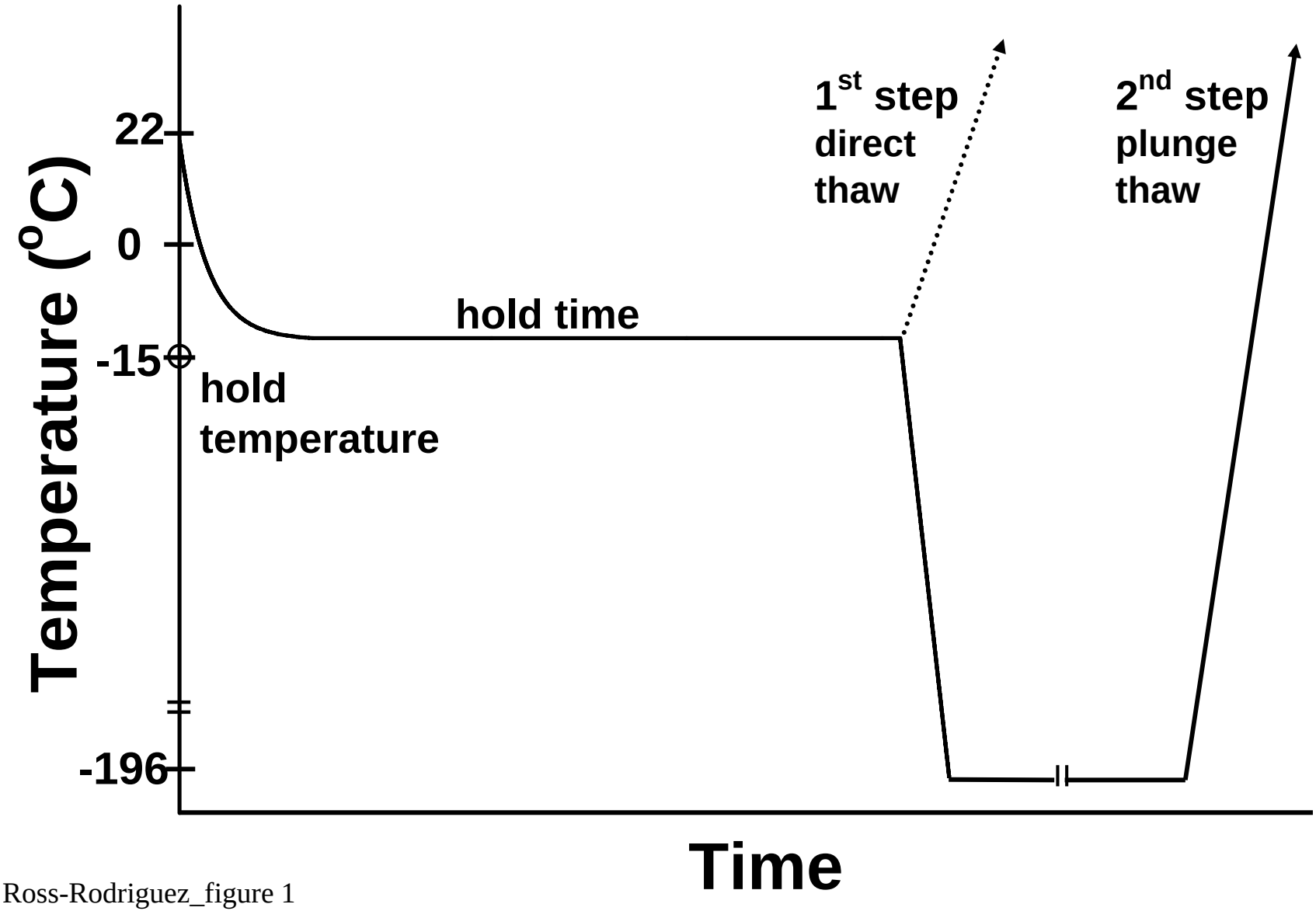

Ross-Rodriguez_figure 1

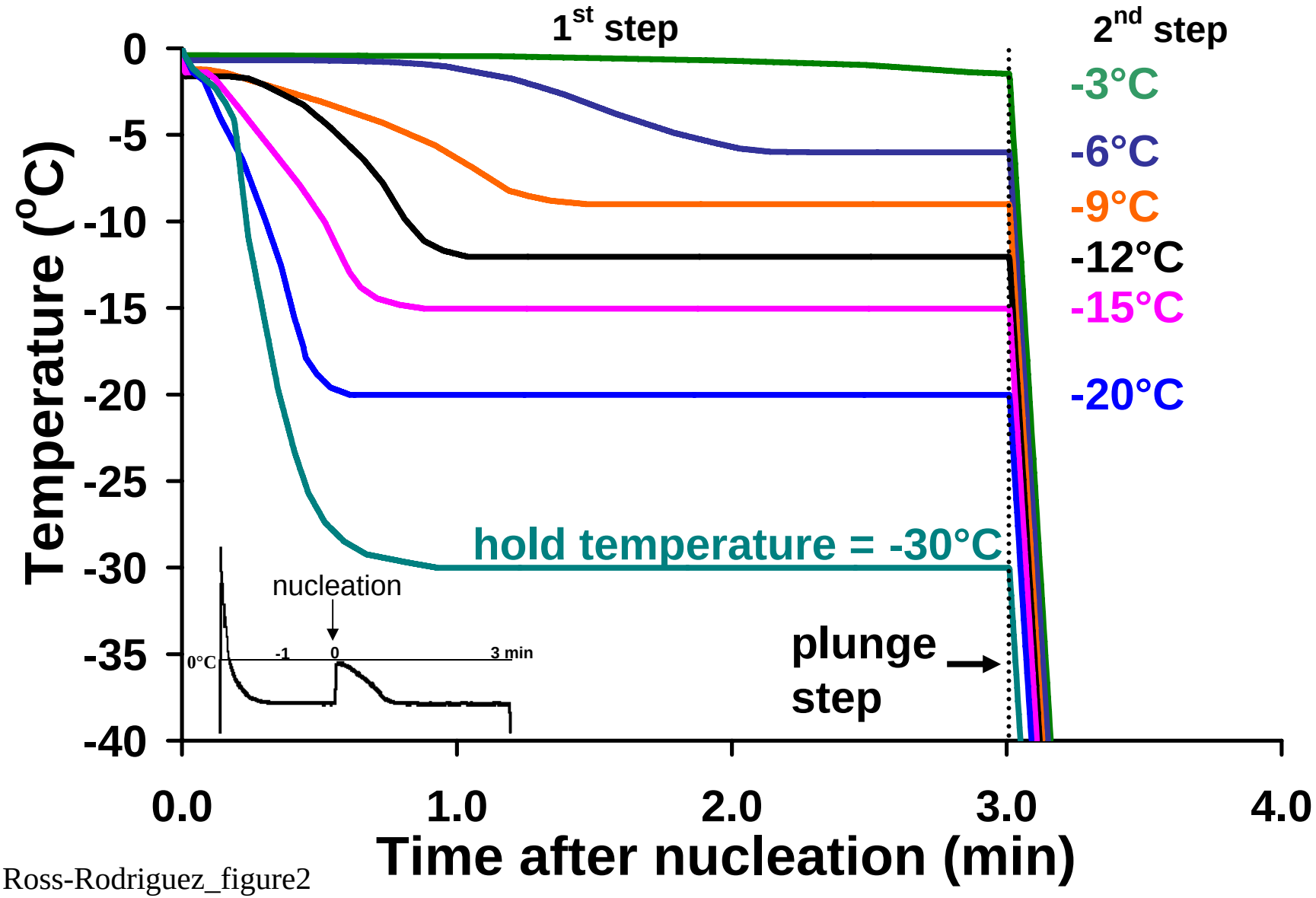

Ross-Rodriguez_figure2

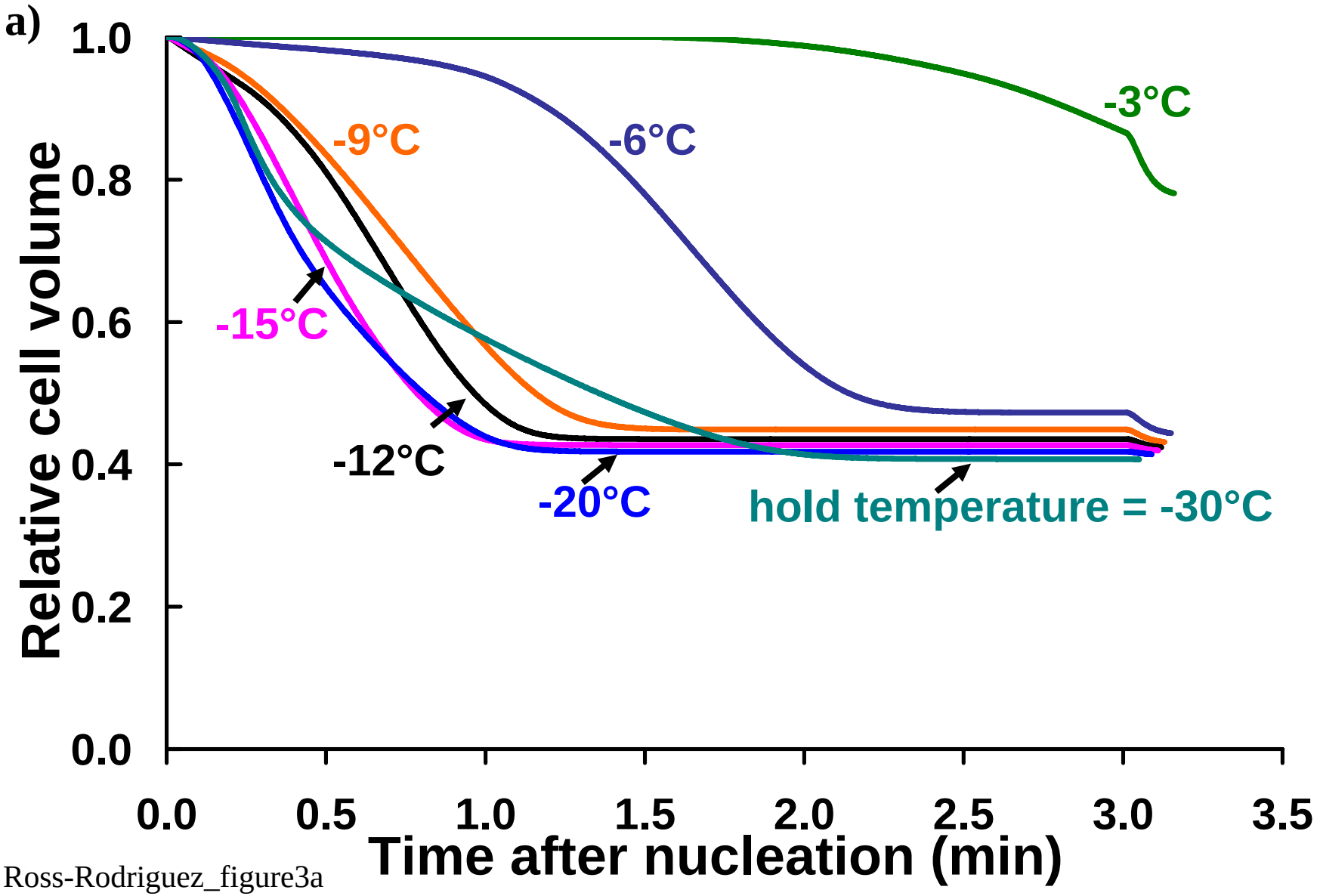

Ross-Rodriguez_figure3a

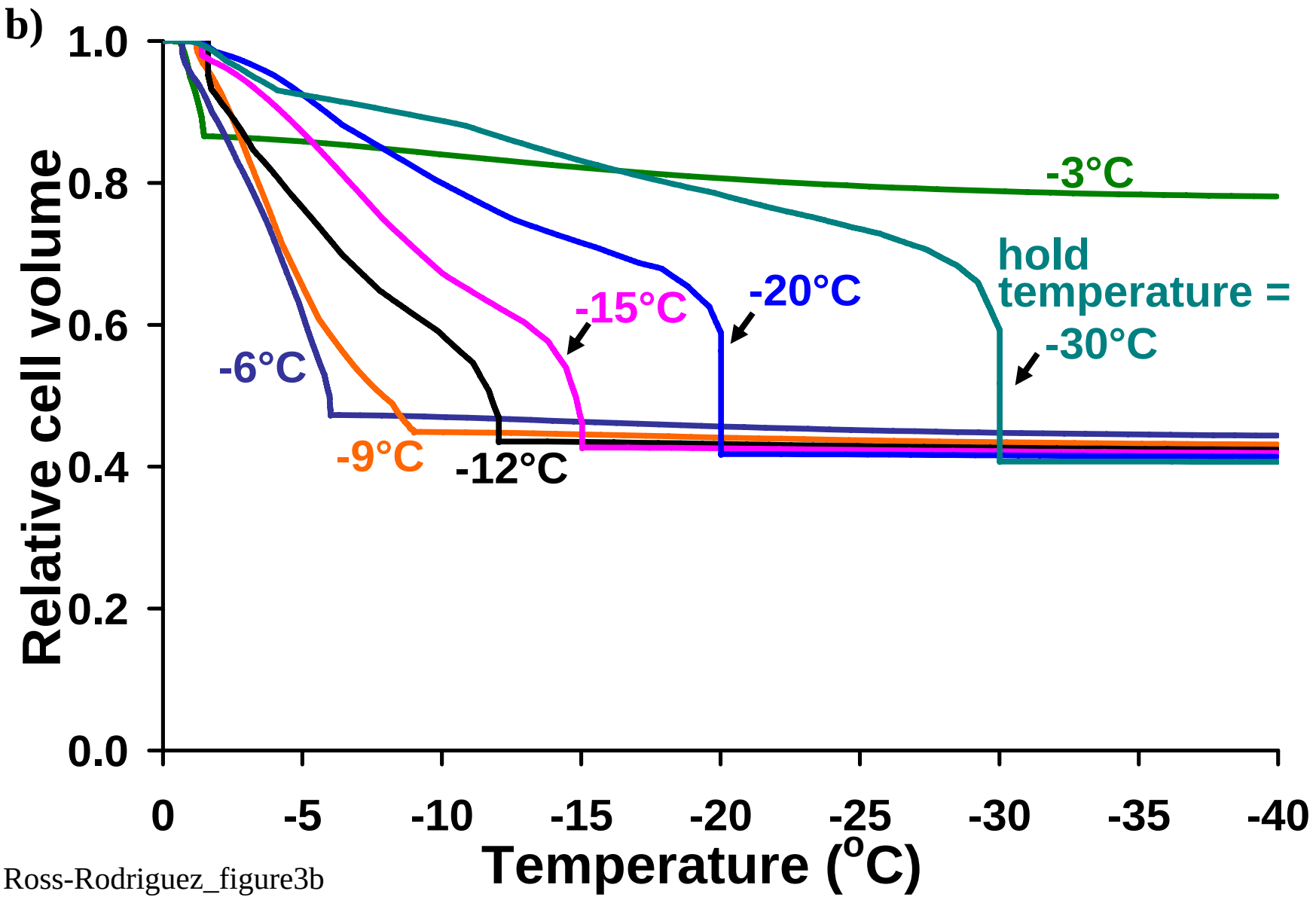

Ross-Rodriguez_figure3b

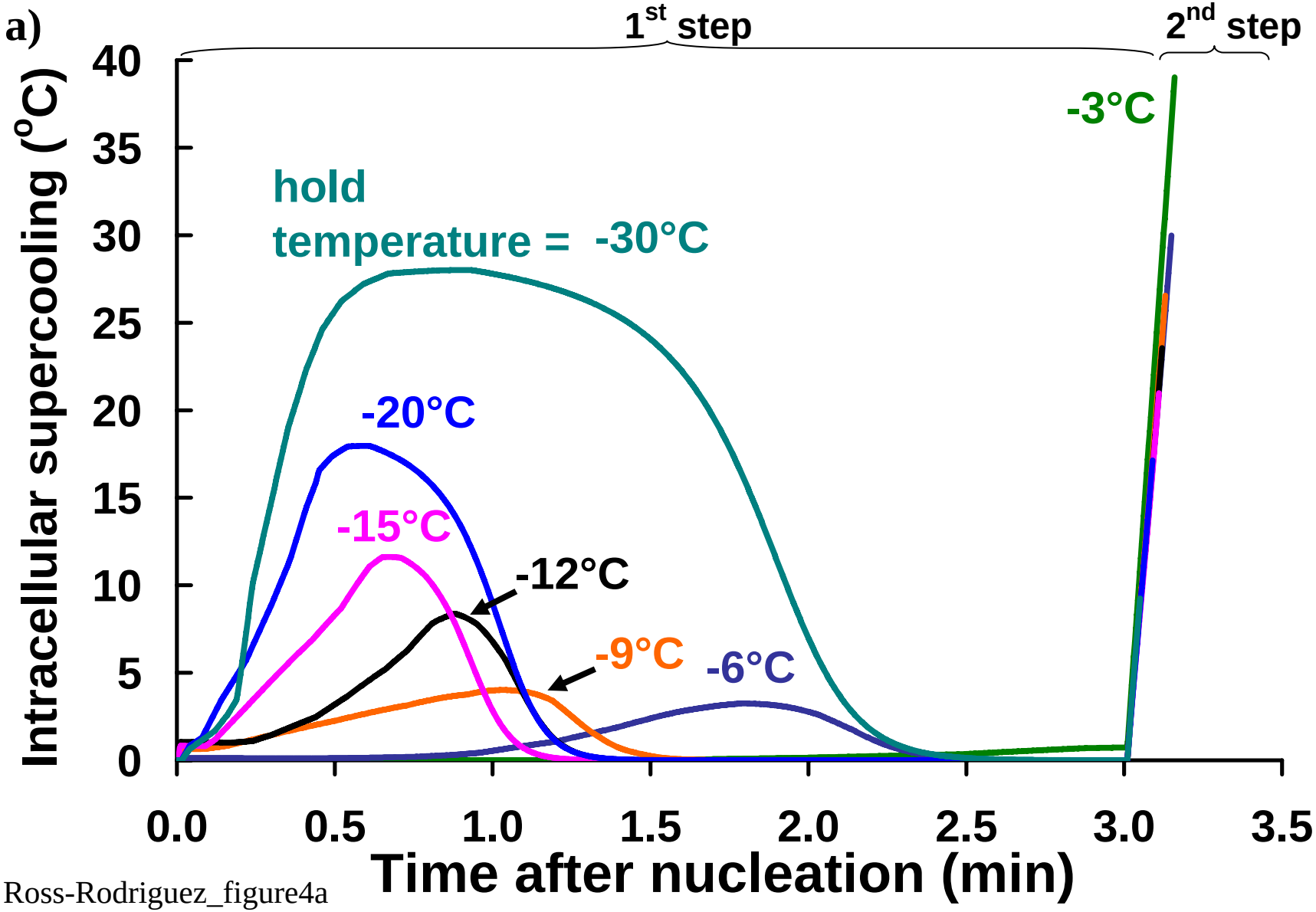

Ross-Rodriguez_figure4a

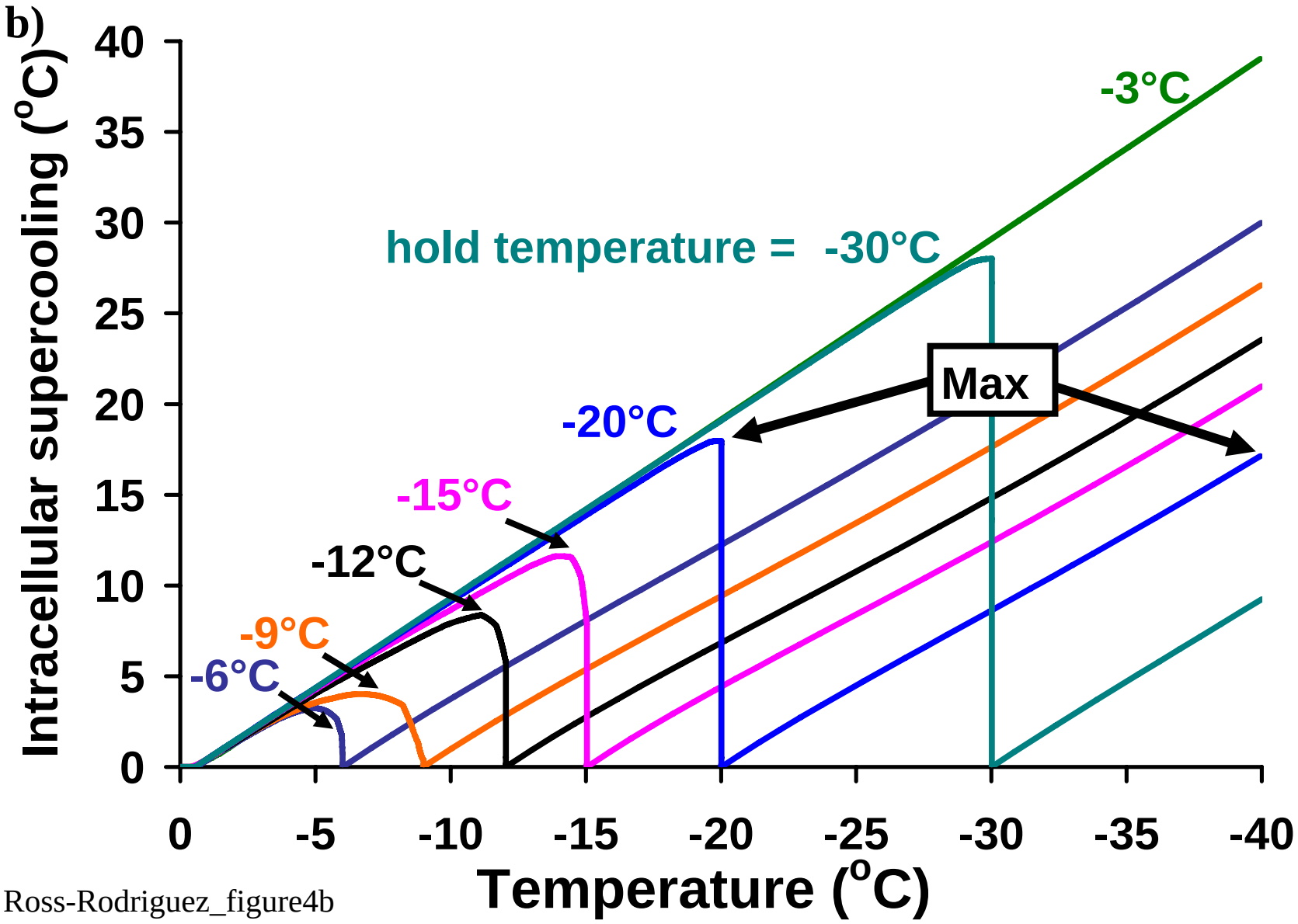

Ross-Rodriguez_figure4b

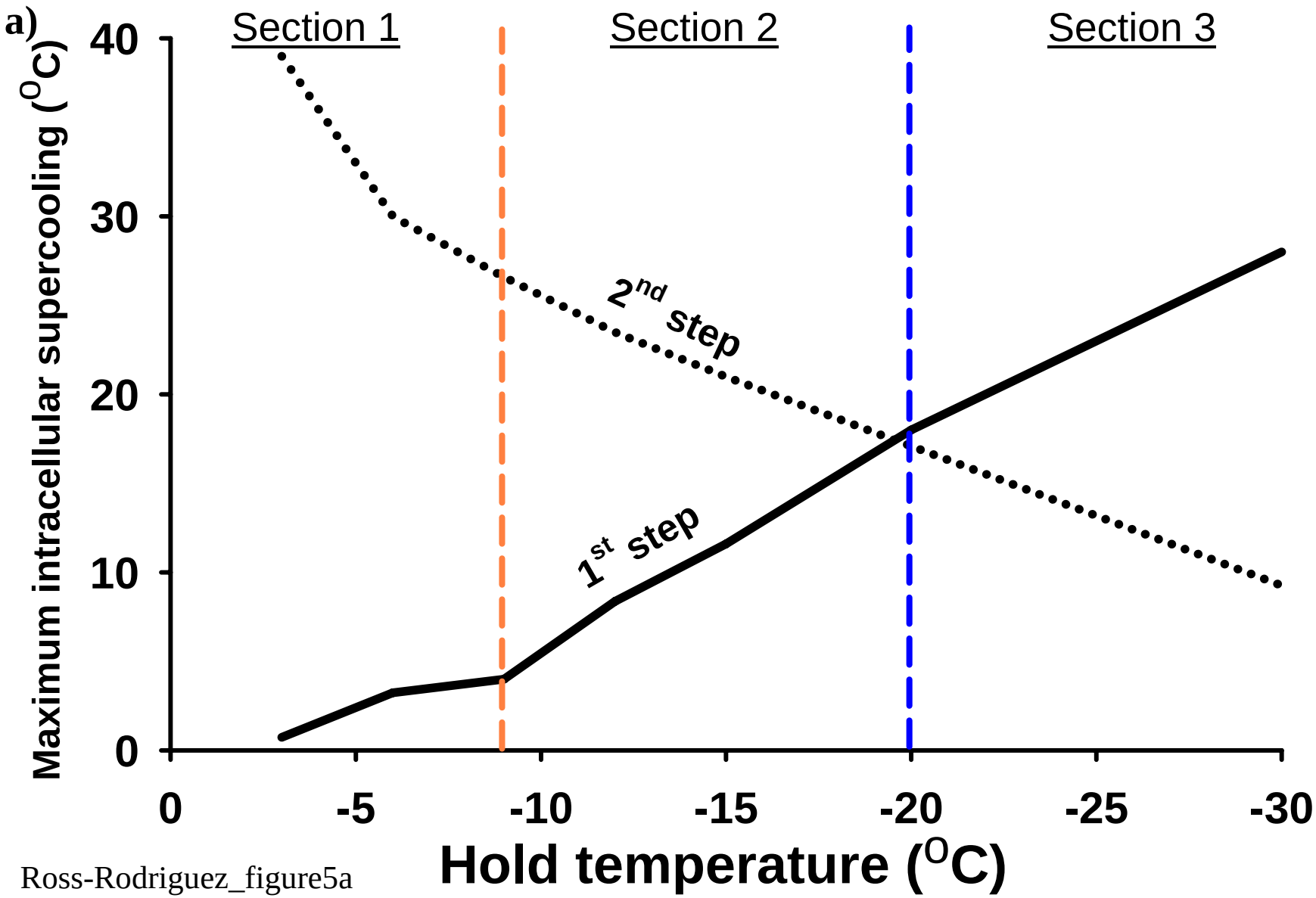

Ross-Rodriguez_figure5a

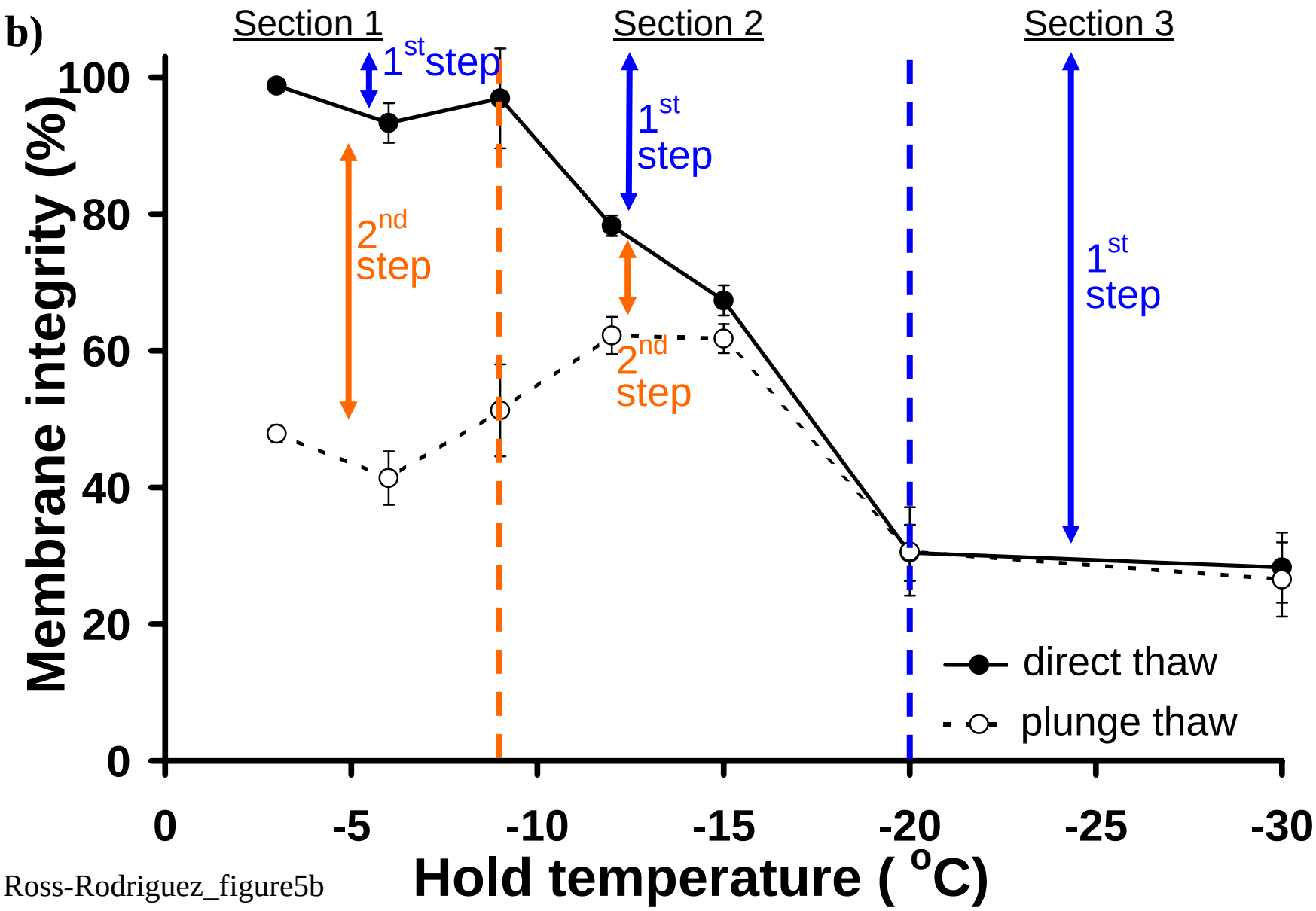

Ross-Rodriguez_figure5b

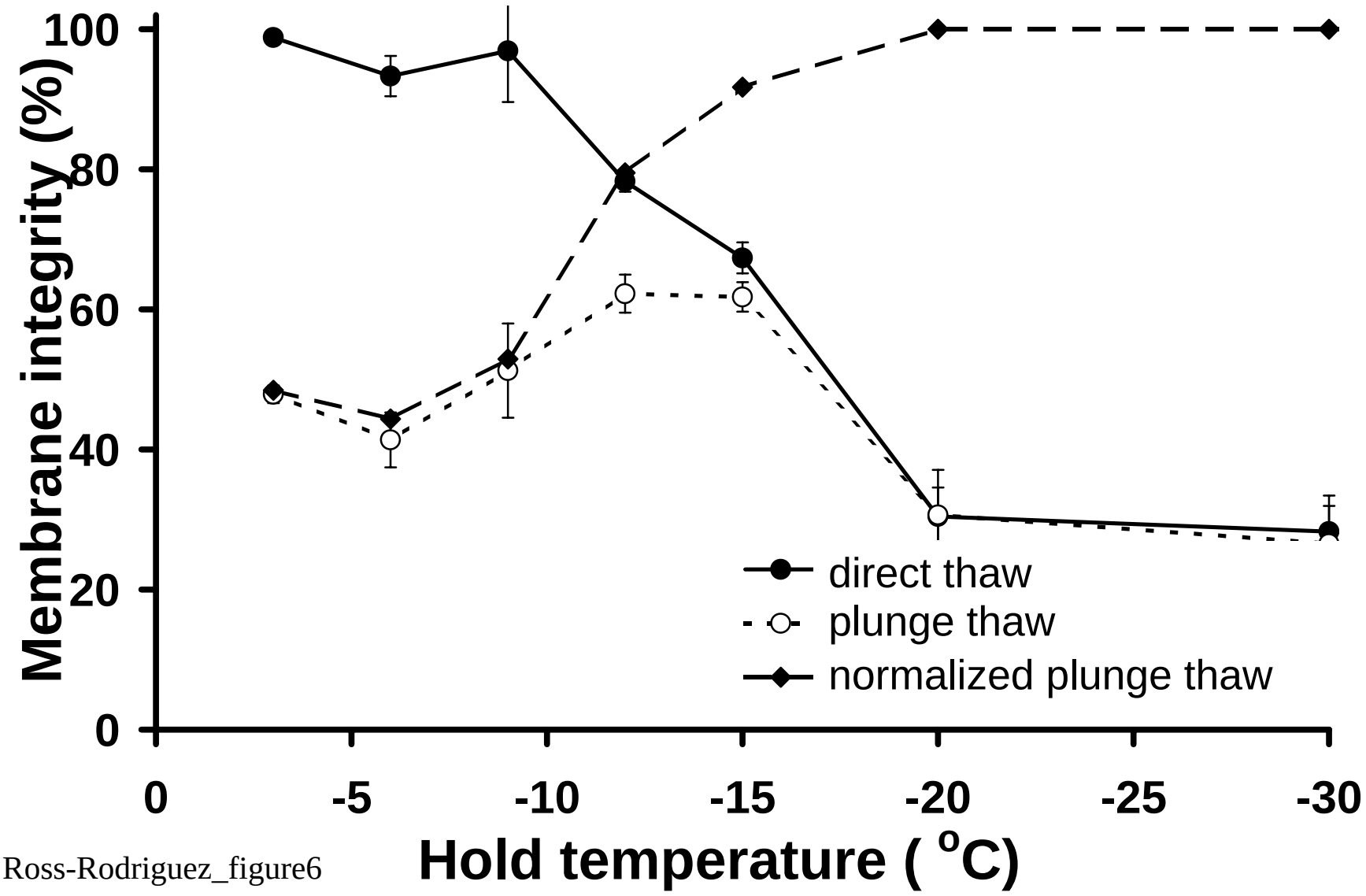

Ross-Rodriguez_figure6

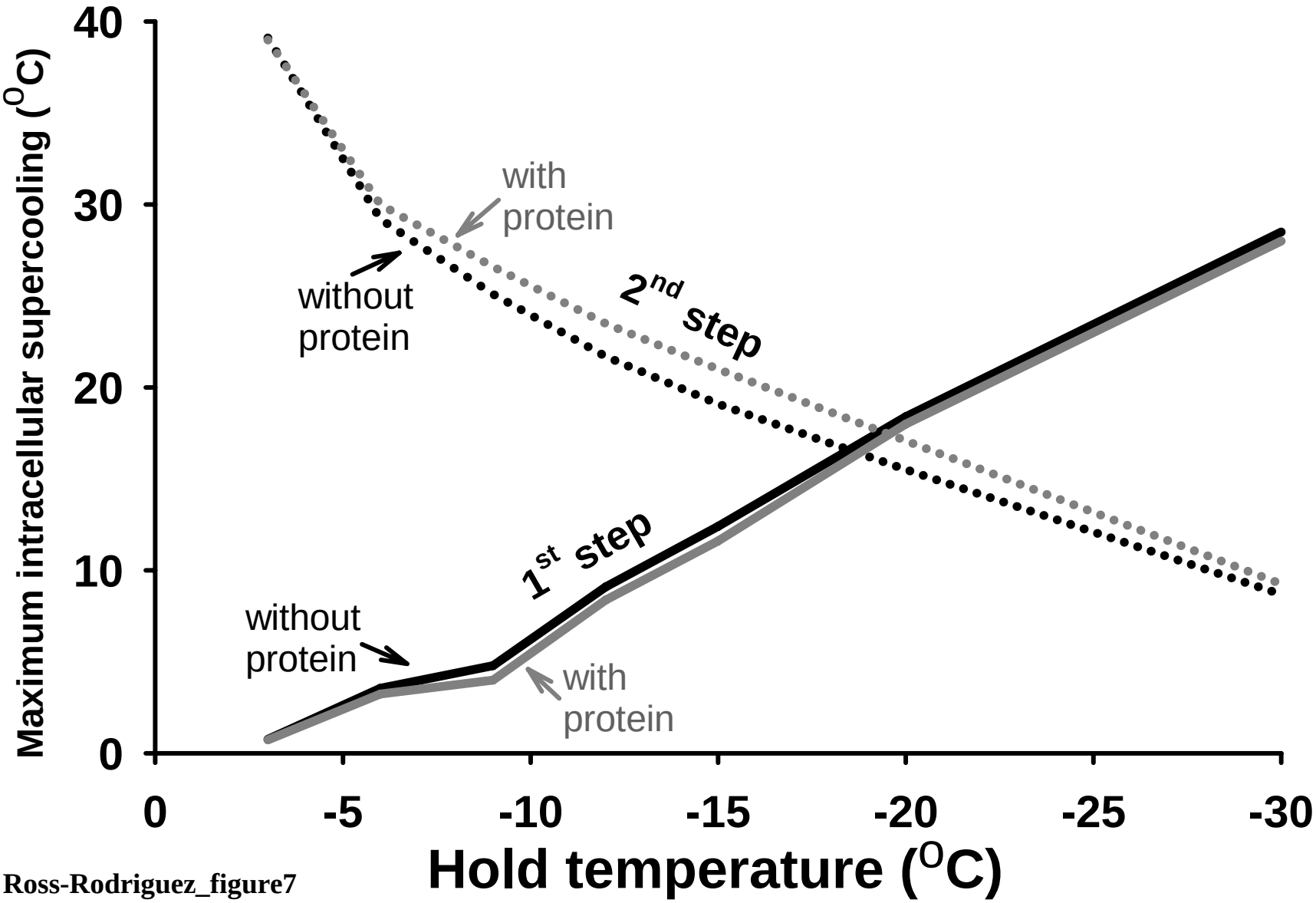

Ross-Rodriguez_figure7

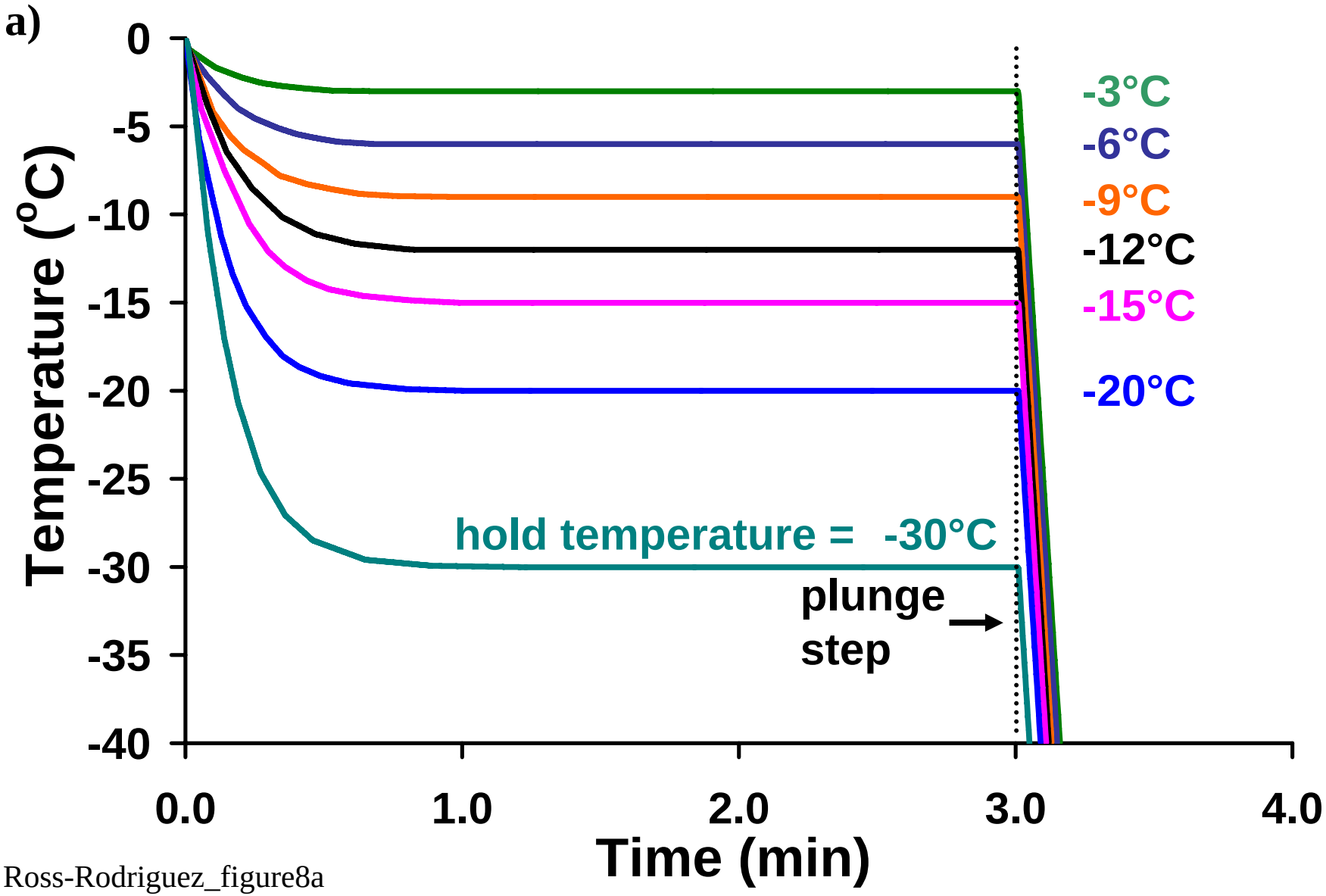

Ross-Rodriguez_figure8a

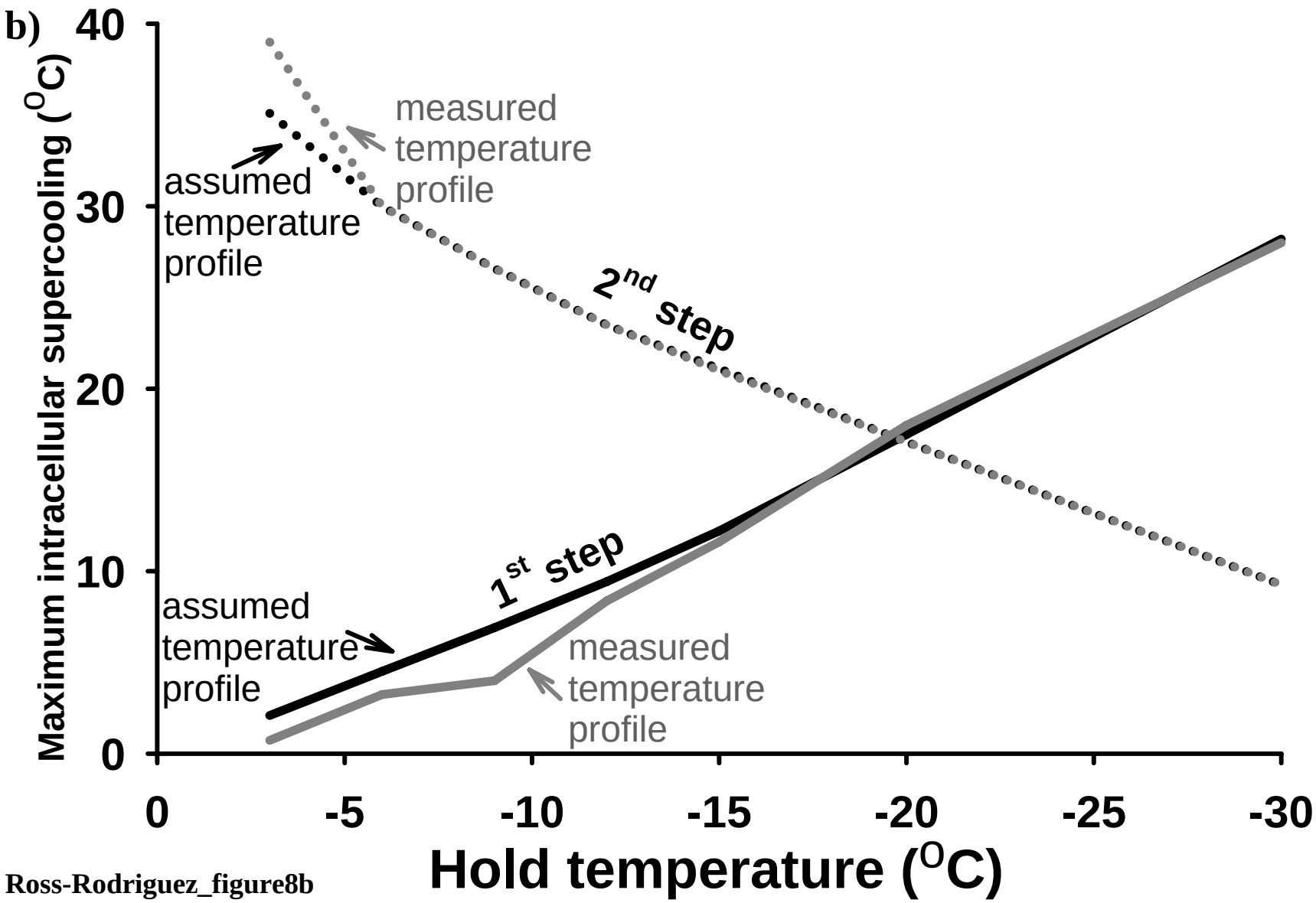

Ross-Rodriguez_figure8b